A coupled dynamic reservoir and pipeline model – development and initial experience

Jan Sagen, Terje Sira and Arild Ek
Institute for Energy Technology
Stig Selberg, Mohamed Chaib and Håvard Eidsmoen
Scandpower Petroleum Technology

1 INTRODUCTION

Field developments are becoming more complex, each facing new and unique challenges, and the importance of understanding the behaviour of the complete system from the reservoir to the receiving facility is increasing. While steady state models of such complete systems are common similar dynamic models have been very rare and their application rather limited [1].

In order to develop an efficient tool for integrated pipeline and reservoir simulations it was determined that a closely linked model was needed to give the required speed and stability. The main emphasis is on the near well bore region and functionality that is important for interaction between the reservoir and the wellbore. This paper focuses on the main features of the reservoir model and how the models are coupled. Simulation examples show interaction effects and experience in working with models extending between different disciplines.

2 INTERACTION BETWEEN RESERVOIR, WELL AND PIPELINE

In general there is a large difference in time scale between typical events in the reservoir, well and pipeline, and most models of production systems from reservoir to receiving facilities are steady state models, where one would typically step through the field life in intervals of a month. This gives sufficient information to determine the depletion of the reservoir, investigate if the field layout is appropriate and perform overall production planning and well allocation. However, there are a number of flow assurance and production issues where dynamic interaction between reservoir and pipeline is important:

- Severe slugging in pipeline and wells causes fluctuations in bottomhole pressure, influencing the inflow from the reservoir. Depending on the characteristics of the near well bore region the variations in the inflow can feed back and aggravate the slugging.
- For low flow rates there can be slow liquid build-up in the well bore, resulting in either the liquid being lifted out of the well as a slug or the well dying.
- During shut-in and packing of pipelines and wells the pressure will build up slowly, the inflow gradually declines and the liquid in the well and pipeline redistributes as the flow stops. The time it takes to reach peak shut-in pressure, the peak pressure and the final

liquid distribution are all important parameters in the design and are strongly influenced both by reservoir and tubing characteristics.

- Following a shut-in it is required that the production can be restarted, and the time to reach normal production should preferably be as short as possible. This can be a challenge in systems with significant redistribution of liquids during a shut-in or when the live fluids are displaced by dead oil during the shut-in for hydrate prevention, and usually detailed re-start procedures are developed.
- During pigging operations lifting the liquid slug in front of a pig out of a high riser can cause significant back-pressure on the reservoir.
- Coning of gas and water in the reservoir causes the reservoir inflow to change with time, significantly changing the characteristics of the flow in the pipeline over time. When breakthrough occurs these changes can be rapid and capturing the details of the well inflow is important.

3 MODEL DESCRIPTION

The following requirements were put forward for the model:

- 1D, 2D and 3D capability in order to cover the range of relevant simulations, from quick screening studies to detailed.
- Should be able to handle four phases, gas, oil, water and solids.
- Future extension to geochemical reactions should be possible.
- Equations and equation solver equal to commercial reservoir software.
- Output formats should be so that industry standard visualization tools can be utilized.
- Computational speed similar to that of the pipeline simulator
- In addition to the black-oil description of the reservoir fluid an option should be available for a fluid description similar to that of the pipeline model. This will also allow the user to select his desired EOS.

3.1 The reservoir model

The black oil model simulates 3-phase fluid transport in porous media. The flow and temperature equations are solved in 1, 2 or 3 dimensions, giving as output saturations, pressures and temperatures in space and time. Input data to the model are permeabilites and porosities of the porous medium, fluid properties of the flowing phases and, if needed, thermal properties of the rock and fluids. In addition boundary conditions at the well and at the outer near well boundary are needed. Typical time-dependent boundary conditions are either injection/production flow rates or pressure, as well as temperature. When coupled to the pipeline model, pressure boundary conditions at the well are defined by this simulator.

The near well model is formulated in a flexible and general manner. The model is capable of handling several types of grids, for instance 1, 2 or 3 dimensional cylindrical or cartesian grid types, and may be extended to handle other grid types as well. The numerical and physical kernel code is not affected by the choice of grid. To achieve numerical stability and robustness, the flow and thermal equations are solved by a fully implicit method. The non-linear equations, described in Appendix A and B, are solved iteratively at each timestep, using a Newton Raphson method.

3.2 Coupling of reservoir model and hydraulic pipeline model

3.2.1 Coupling algorithm

For practical purposes the reservoir model is considered as a plug-in to the pipeline model, and it is only started and used as determined by the input to the pipeline model. The dll containing the reservoir model is then loaded automatically and the required connections between the pipeline model and reservoir model are automatically created.

The flow from the reservoir model is defined by matching up the boundary condition of elements of the reservoir grid with inflow points in the pipeline. The basic principle is that the pipeline model provides the pressure boundary for the reservoir model while the reservoir model provides the flow into the pipeline together with the fluid temperature. Since both the reservoir model and the pipeline models are three phase the phase fractions must also be provided. A complicating factor is that the flow can be in both directions, which is the case for injection wells but could also be the case for certain transient events in a production well. However this is captured within the coupling scheme.

Assuming the models have been integrated up to time step n, the implicit numerical coupling algorithm is outlined in the three steps below. Whenever the models need mass fractions (in case of inflow relative to each model), the latest values of these variables are used. Whenever new values are calculated, these are made available for both models.

Step 1: The pipeline model begins integration to time step n+1 by requesting the reservoir model to calculate coefficients as defined in equation (3.1)

$$Q_i^{n+1} = a_i P_{bh,i}^{n+1} + b_i \quad \textbf{(3.1)}$$

where $P_{bh,i}^{n+1}$ is the pressure in the relevant control volume in the pipeline model and Q_i^{n+1} is the mass flow rate for each phase. The explicit method is a special case of the implicit coupling, setting $a_i = 0$ and leaving b_i equal to the flow rate from the reservoir simulator.

Step 2: The pipeline model uses equation (3.1) as a boundary condition and solves the complete flow network. The pipeline model has then completed time step n+1 and transmits $P_{bh,i}^{n+1}$ and Q_i^{n+1} back to the reservoir simulator.

Step 3: The reservoir model completes the time step by using the computed values from the pipeline model as boundary condition.

3.2.2 Calculation of the coefficients a_i and b_i

Since we do not know the n+1 solution in Step1 described in section 3.2.1, the coefficients a_i and b_i are estimated at the previous timestep n. Mathematically, the expressions for a_i and b_i may be written:

$$a_i = \frac{dQ_i^n}{dP_{bh,i}^n} \qquad (3.2)$$

$$b_i = Q_i^n - a_i P_{bh,i}^n \quad (3.3)$$

where Q_i^n and $P_{bh,i}^n$ have been calculated at the old timestep n. Hence the calculation of b_i by (3.3) is simple once the coefficient a_i has been calculated. a_i may be interpreted as the overall reservoir model sensitivity of the mass flowrate with respect to the boundary pressure, and can be derived analytically from the reservoir equations given in Appendix A. However, the details of this derivation will not be discussed here.

We will now adopt some simplifications which in the end lead to a method of choosing the level of implicitness in the coupling. Figure 1 shows a sketch of three different grid block domains related to the specific boundary. The coefficients a_i and b_i are estimated using a method where the level of implicitness is defined as a natural number ≥ 0. The level parameter may be given as part of the model input, or one can imagine that the model itself could determine dynamically what level of implicitness is needed at a specific timestep.

Figure 1 illustrates a 2D example, but the method is equally applicable in 3D. Furthermore, the figures show a one-to-one correspondence between control volumes in the well simulator and the nearwell simulator. The method is equally applicable when this is not the case. As before we consider a specific boundary with bottomhole pressure P_{bh}. The level 1 domain is defined as a set consisting of one grid block, namely the nearest neighbour to the boundary. The level 2 domain is the set consisting of all the grid blocks being neighbours to this block. For each increase of the level number, a new generation of neighbour blocks is included in the set (in 3D). In principle, the sensitivity coefficient a depends on the behaviour of all the grid blocks in the reservoir. We now assume a fixed level of domain and calculate the sensitivity assuming that only the solution inside the domain is affected by the varying bottomhole pressure. Outside the border of the domain, we assume that the pressure and saturations are kept fixed at values from the previous timestep.

4 SAMPLE PROBLEMS

4.1 Start-up with gas coning and slugging

The aim of this case is to illustrate how the changes of the gas oil ratio during a start-up of a well, due to gas coning, could significantly influence the slugging characteristics of a pipeline. Further, the aim is to illustrate how the inclusion of the reservoir model would influence the results compared to what the typical pipeline model would give.

The profile of the well and pipeline is shown in Figure 2. The well has a total depth of 3300 m and a 0.1143 m (4.5”) tubing ID. The wellhead is at approximately 1500 m water depth and a slightly downward inclined 0.2222 m (8”) ID pipeline extends 8 km to the base of a 0.1524 m (6”) ID catenary riser. The downward sloping pipeline profile is fairly typical of deepwater developments, but is also selected because it is known to cause slugging problems. The pressure in the receiving facility is 8.3 MPa and for simplicity we assume that the well and pipeline are gas filled at start-up.

The description of the reservoir model is given in Figure 3. The reservoir is assumed to be 90 meter thick of which the gas cap is the upper 30 meter. The reservoir model assumes radial symmetry, is divided in 10 layers in radial direction (automatically calculated by the model)

and constant pressure and temperature is imposed as a condition on the outer boundary (66°C and 55.0 MPa). Production occurs from a 30 meter thick zone in the middle of the reservoir. The permeability in the reservoir is 13 mDarcy and the porosity 0.2.

Figure 4 shows the total mass flow rate and the gas mass flow in the wellbore just above the production zone for the first 36 hours of production. We see that while the oil production stays relatively constant the gas production increases significantly. When considering the oil saturation in the reservoir after 36 hours, shown in Figure 3, we can see that the gas cones into the production zone causing this increase in gas production. The variations in flow rate are caused by variations in the bottomhole pressure, shown in Figure 5. These variations are caused by terrain slugging in the riser. The total liquid production into the platform is shown in Figure 6. At the end of the 36 hour period shown here sufficient gas has reached the riser for the slugging to stop, and the flow stabilizes.

When considering the radial pressure profile in the reservoir at the end of the 36 hour period only in the inner 15 m towards the wellbore is the pressure significantly lower than 55 MPa, meaning that it was not necessary to extend the model out to 300 m for this case.

It is interesting to investigate how these results compare to how a start-up simulation would have been performed without a near wellbore model. Typically production rates would have been supplied by the reservoir group at certain time point and a linear production index and a gas fraction would have been computed based on these data. As a comparison a linear production index was computed to match the conditions at 36 hours in the current simulation.

Figure 5 through Figure 7 shows a comparison of the results obtained with the two models, for liquid flow rate into the reservoir, gas rate from the production zone and bottomhole pressure. As expected the results are similar at the end of the 36 hours, where the production index was matched to the wellbore inflow data, however the model with the linear production index shows no slugging. The main reason for this is that for the linear production index the gas ratio from the well is constant, and the initial gas rate is significantly larger than what it should have been.

4.2 Start-up and shut-in of horizontal well

A second simulation has been performed to illustrate a start-up and shut-in of a horizontal well. The well trajectory is shown in Figure 8. The total depth of the well is 2500 m and there is a 500 m long horizontal section. The reservoir extends 400 m from the end of the wellbore and a cross section of the reservoir is shown in Figure 11. The figure also indicates how the reservoir is discretized (19 cells in y-direction, 13 in z-direction and 8 in x-direction). The well is located along the x-axis in the middle of the reservoir in the y- and z-direction and there are 8 inflow points distributed evenly along the wellbore. In the y and z directions the grid spacing has been reduced around the wellbore in order to get a better description of the inflow, especially during transients.

The initial pressure is 40 MPa and there is a 15 m thick gas cap. The horizontal part of the wellbore is liquid filled and the vertical part is gas filled. The wellhead valve is closed and the downstream pressure is 15 MPa. In this case the outer boundaries of the reservoir are assumed to be closed, so we would expect the pressure in the reservoir to drop during the simulation. The permeability in the reservoir is 13 mDarcy and the porosity 0.2.

Figure 9 shows the gas mass flow and the total mass flow at the end of the horizontal section of the wellbore representing the total flow from the reservoir. Initially there is only liquid flow, but after 10 hours gas from the gas cap reaches the well and free gas is produced.

The bottomhole pressure is shown in Figure 10. When the wellhead valve is opened the bottom hole pressure drops down to almost 15 MPa, since there is only gas in the vertical part of the wellbore. The pressure then increases to 35 MPa as the vertical part of the wellbore is filled with liquid and then decreases again as the well starts producing gas. Figure 10 also shows the liquid rate at the wellhead, and we notice that when gas production start the liquid rate increases. When gas is produced the liquid head in the well is reduced, resulting in larger drawdown and an increase in the total production from the well. Following the shut-in the pressure does not return to the original pressure of 40 MPa. Since our reservoir is a closed in volume the pressure drops as the reserves are produced. Due to the relatively small volume of the gas cap the pressure drops almost 0.7 MPa during this simulation. Another important parameter that can be determined from Figure 10 is the shut-in wellhead pressure. The pressure transient is determined by the dynamics of both the wellbore and the reservoir and the correct rate of pressure build-up can only be determined by a coupled model.

Figure 11 shows the oil saturation in a cross-section of the reservoir just before the shut-in. Notice the gas coning towards the reservoir which explains the increase in gas flow observed after the initial phase of single phase oil production.

5 LESSONS LEARNED AND FURTHER DEVELOPMENT

Following the initial testing of the model and discussions between reservoir and flow assurance engineers a number of issues have been identified on how the different disciplines work, which needs to be taken into consideration in the future model development. A number of issues where especial care needs to be paid when performing these types of simulations have been identified.

Model set up with regards to fluid boundary conditions are very different for reservoir simulations and pipeline simulations. Pipeline models are usually set up with a specified gas, oil and water fraction at the inflow point, representing the inflow from the reservoir at a certain point in time. In the reservoir model this is a result of three dimensional flows of the different phases over time. In general it is simple to set up a pipeline model based on the input from the reservoir, since only a few parameters are required. However, back calculating reservoir conditions that produce a set of pipeline flow rates is very difficult. It is thus difficult for a pipeline engineer to create a reservoir model that gives a specific inflow.

Building reservoir models is a complex exercise and this is outside the scope of what pipeline engineers could be expected to do. Thus it would be a significant benefit if a model, or part of a model, made by a standard reservoir modelling tool could be imported and used directly. This would make it possible for a pipeline engineer to take a model developed by a reservoir engineer as input to the coupled simulation.

Since it is not realistic to run such a coupled model for the whole field life it is required that typical conditions over the field life can be generated as starting conditions for these coupled runs. This could be done in different ways. The two models could be run separately and then coupled at the desired time, where the reservoir model could typically run with very long time

steps to speed up the process. Alternatively the reservoir model could be initialized with a sub-set of the conditions from a larger reservoir model at a desired time. I.e. the initialisation of the reservoir should be possible based on the results from industry standard reservoir models. If only a sub-set of a complete reservoir model is used for the near wellbore model the boundary conditions should also be on such a form that they can be copied from the results from the larger model.

Test cases have been run to check the sensitivity of the flow into the well w.r.t. the reservoir grid. The experience is that the results can depend quite significantly on the grid even for grids that are relatively fine compared to what is typical for reservoir simulations. Guidelines on making proper grids in the near wellbore region will be developed.

An old but persistent problem facing the oil industry is the formation of mineral scales from produced water/brines in oil/gas wells and pipelines. Lost production, formation damage and operational expenses caused by scale deposits is a severe problem today. By making a near well zone scaling/inhibitor tool available in the state-of-the-art multiphase flow simulator, challenging problems related to scale formation/scale inhibition in the near well zone may be addressed.

6 CONCLUSIONS

A coupled reservoir and pipeline model has been developed where the simulation speed is such that dynamic simulations of days or weeks can easily be performed, and the simulation speed of the reservoir model is of the same order as the pipeline model. Further, the method for coupling the models has been shown to be stable and working for both production and injection.

Simple case studies have been used to illustrate the importance of the interaction between the near reservoir region and the pipeline due to such effect as gas coning and bottomhole pressure oscillations. However, so far it has not been possible to obtain data sets that can be used to verify the complete model against measured data. Work continues on trying to achieve this.

7 ACKNOWLEDGEMENTS

The authors would like to thank the sponsors of the Horizon project (Chevron, ENI, ExxonMobil, Hydro, Shell and Statoil) for permission to publish this paper.

8 REFERENCES

1. Ballard, A.L., Adeyeye, D., Litvak, M., Wang, C.H., Stein, M.H., Cecil, C. and Dotson, B.D.: Predicting Highly Unstable Tight Gas Well Performance, SPE 96256, SPT ATCE, Dallas, Texas, US, 9-12. October 2005
2. A.T. Watson, Sensitivity Analysis of Two-Phase Reservoir History Matching, SPE Reservoir Engineering, Vol. 4, No. 3, 1988, pp. 319-324.

9 APPENDIX A RESERVOIR MODEL EQUATIONS

Water equation

$$\frac{\partial}{\partial t}(b_w \varphi S_w) + \nabla \cdot (b_w \underline{u}_w) = q_w \quad \text{(A.1)}$$

Oil equation

$$\frac{\partial}{\partial t}(b_o \varphi S_o) + \nabla \cdot (b_o \underline{u}_o) = q_o \quad \text{(A.2)}$$

Gas equation

$$\frac{\partial}{\partial t}(b_g \varphi S_g + R_S b_o \varphi S_o) + \nabla \cdot (b_g \underline{u}_g + R_S b_o \underline{u}_o) = q_{gphase} + q_o \cdot R_S \quad \text{(A.3)}$$

where the Darcy velocities are given by

$$\underline{u}_w = -K \frac{kr_w}{\mu_w}(\nabla p_w - \rho_w \mathbf{g}) \quad \text{(A.4)}$$

$$\underline{u}_o = -K \frac{kr_o}{\mu_o}(\nabla p_o - \rho_o \mathbf{g}) \quad \text{(A.5)}$$

$$\underline{u}_g = -K \frac{kr_g}{\mu_g}(\nabla p_g - \rho_g \mathbf{g}) \quad \text{(A.6)}$$

Closure relation

$$S_w + S_o + S_g = 1 \quad \text{(A7)}$$

Energy equation:

$$\frac{\partial}{\partial t}(b_w \varphi \rho_{w,STC} S_w u_w + b_o \varphi \rho_{o,STC} S_o u_o + b_g \varphi \rho_{g,STC} S_g u_g + R_S b_o \varphi \rho_{o,STC} S_o u_o + (1-\varphi)\rho_s u_s)$$

$$+ \nabla \cdot (b_w h_w \rho_{w,STC} \underline{u}_w + b_o h_o \rho_{o,STC} \underline{u}_o + b_g h_g \rho_{g,STC} \underline{u}_g + R_S b_o h_o \rho_{o,STC} \underline{u}_o) + \nabla \cdot (k_T \nabla T) + Q_{loss} =$$

$$Q_w + Q_o + Q_{gphase} + Q_o \cdot R_S \quad \text{(A.8)}$$

.

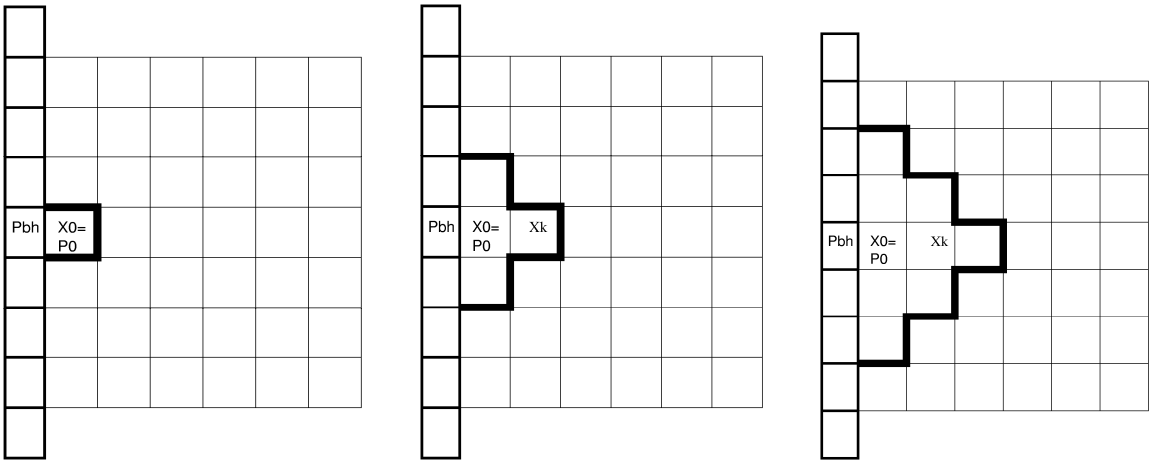

Figure 1. From left to right level 1 domain, level 2 domain and level 3 domain coupling.

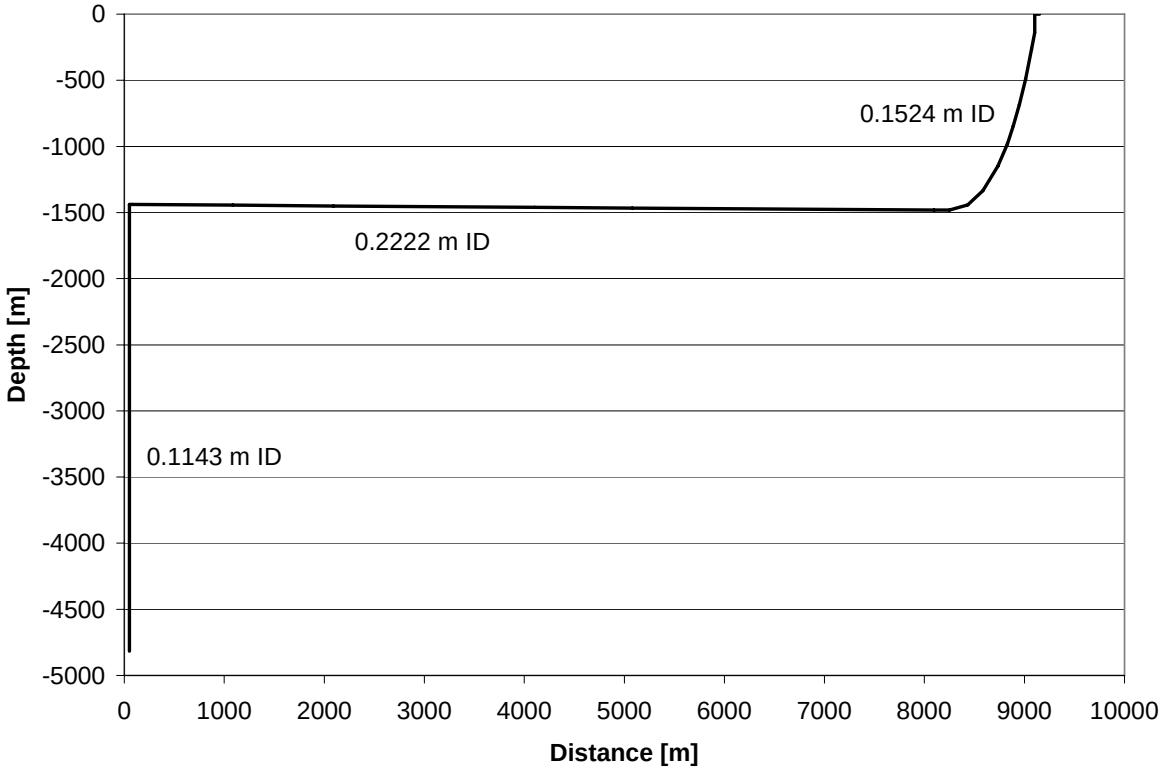

Figure 2. Schematic description of well and pipeline profile.

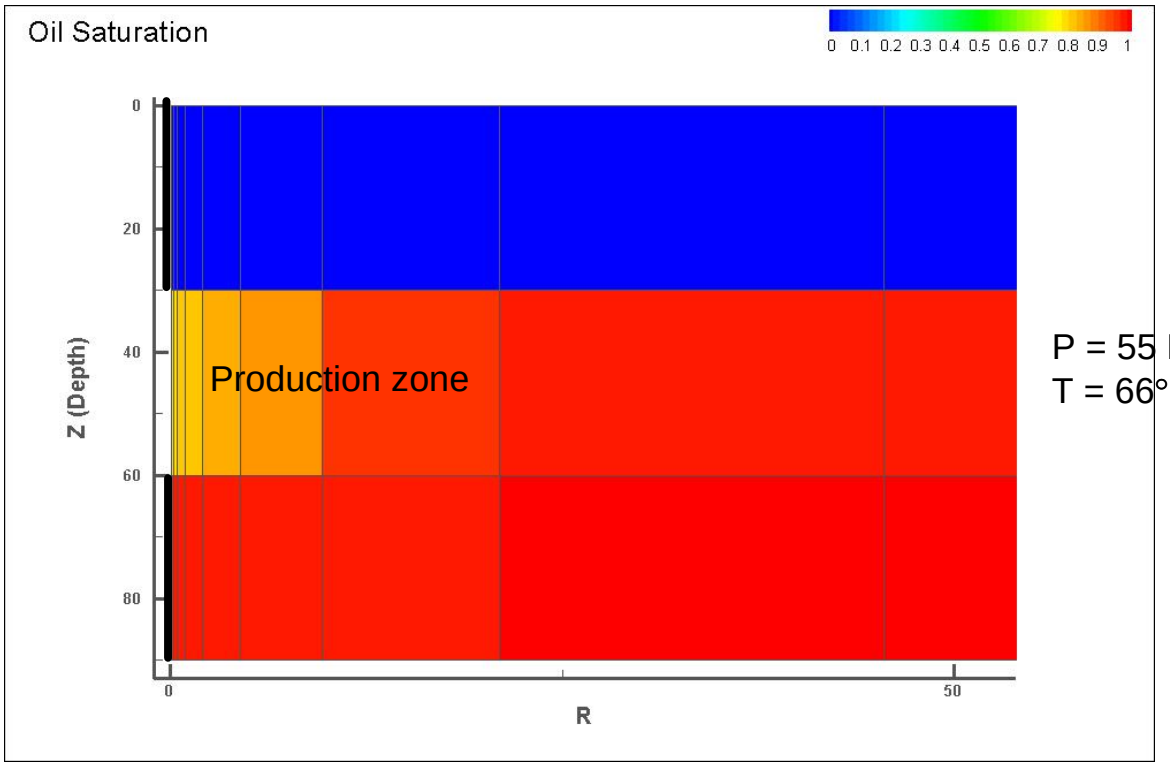

Figure 3. Schematic description of reservoir model and the oil saturation at 36 hours.

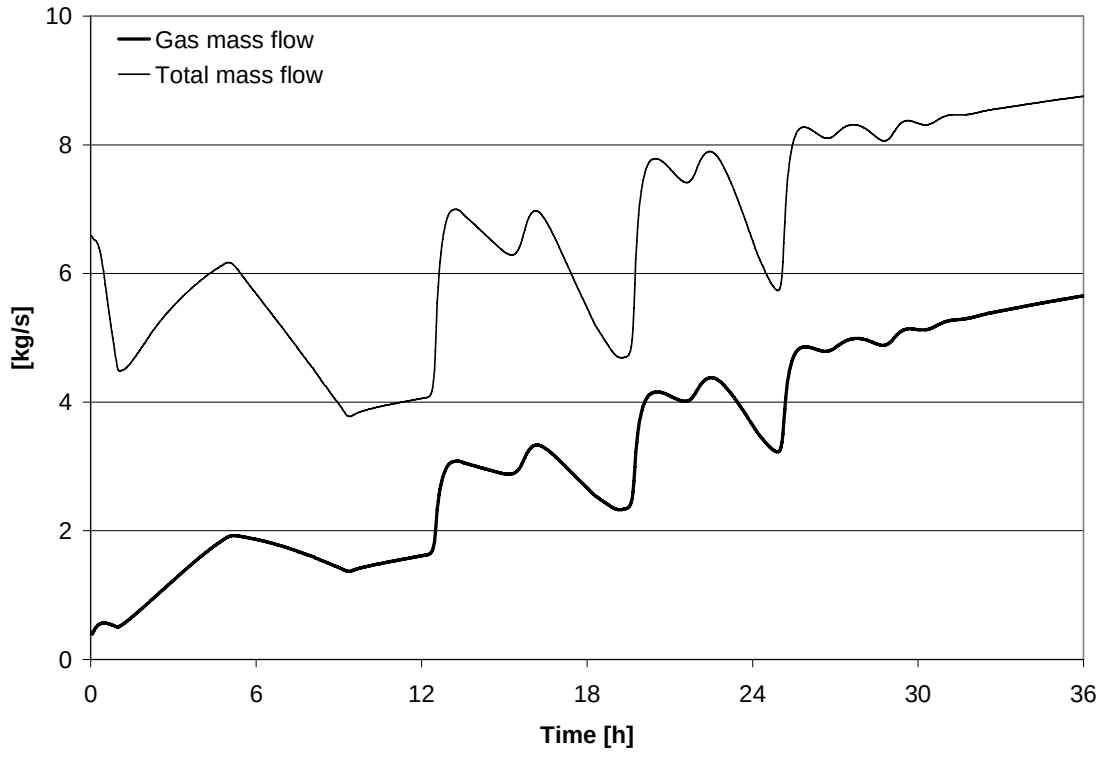

Figure 4. Gas mass flow and total mass flow in the well just above the reservoir.

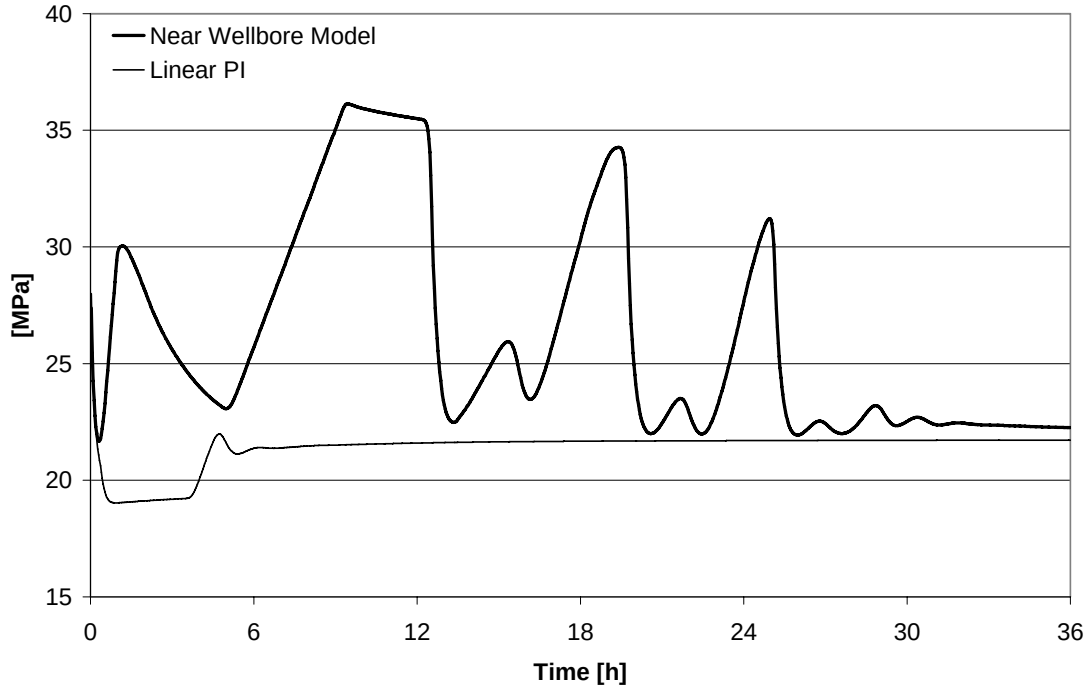

Figure 5. Comparison of bottomhole presser for model with near wellborn reservoir model and linear PI inflow model.

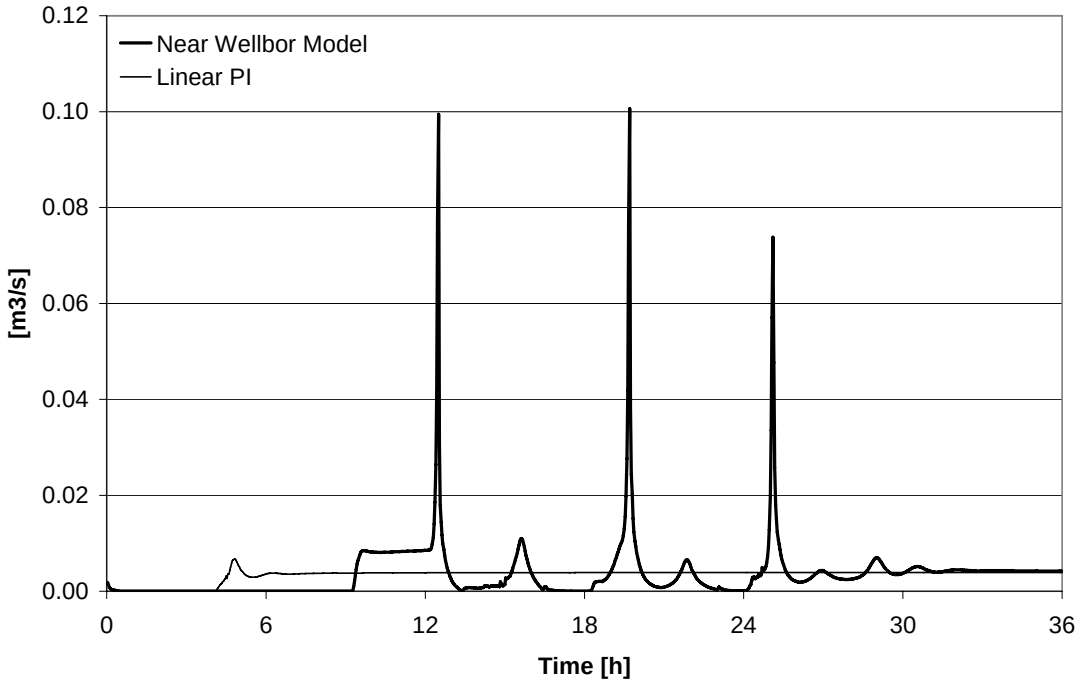

Figure 6. Comparison of liquid production rate into platform for model with near wellbore reservoir model and linear PI inflow model.

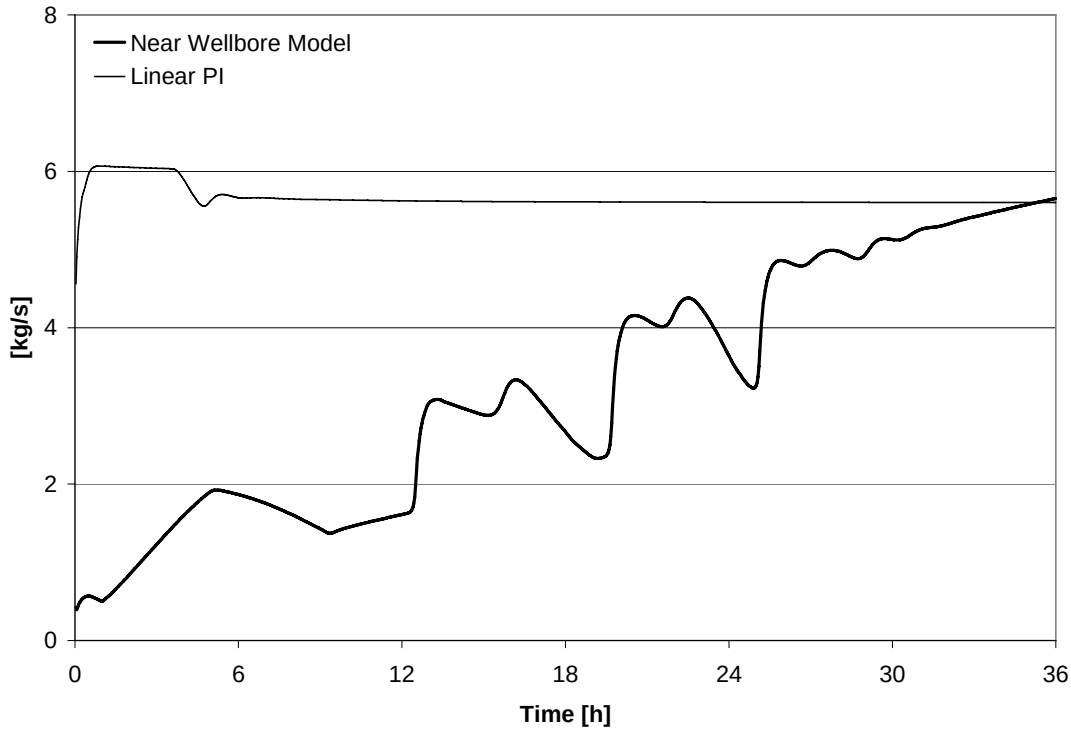

Figure 7. Comparison of gas production rate from model with near wellborn reservoir model and linear PI inflow model.

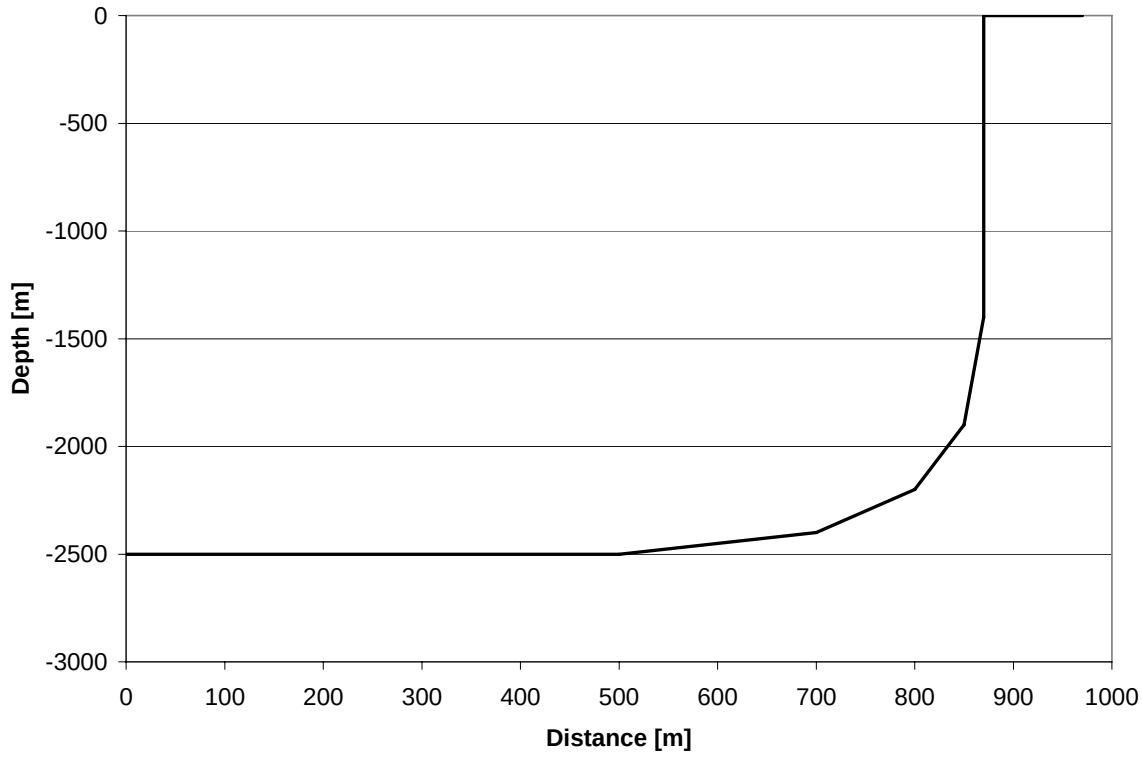

Figure 8. Wellbore profile.

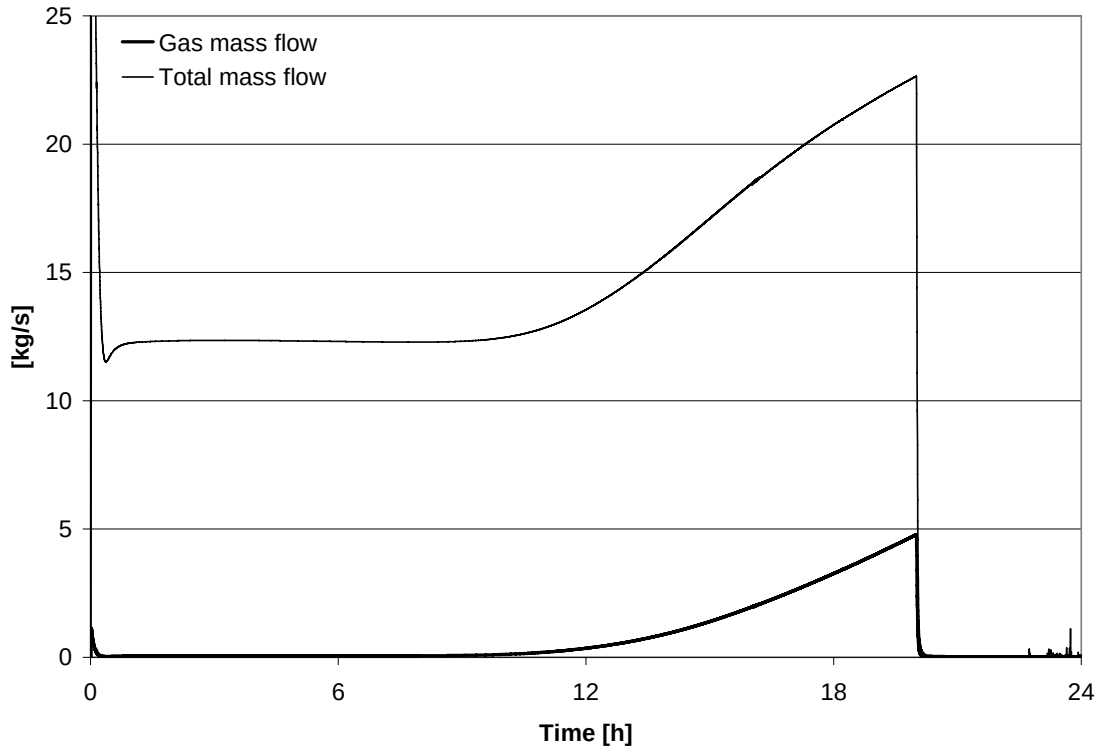

Figure 9. Gas mass flow and total mass flow in well bore at outlet of production zone.

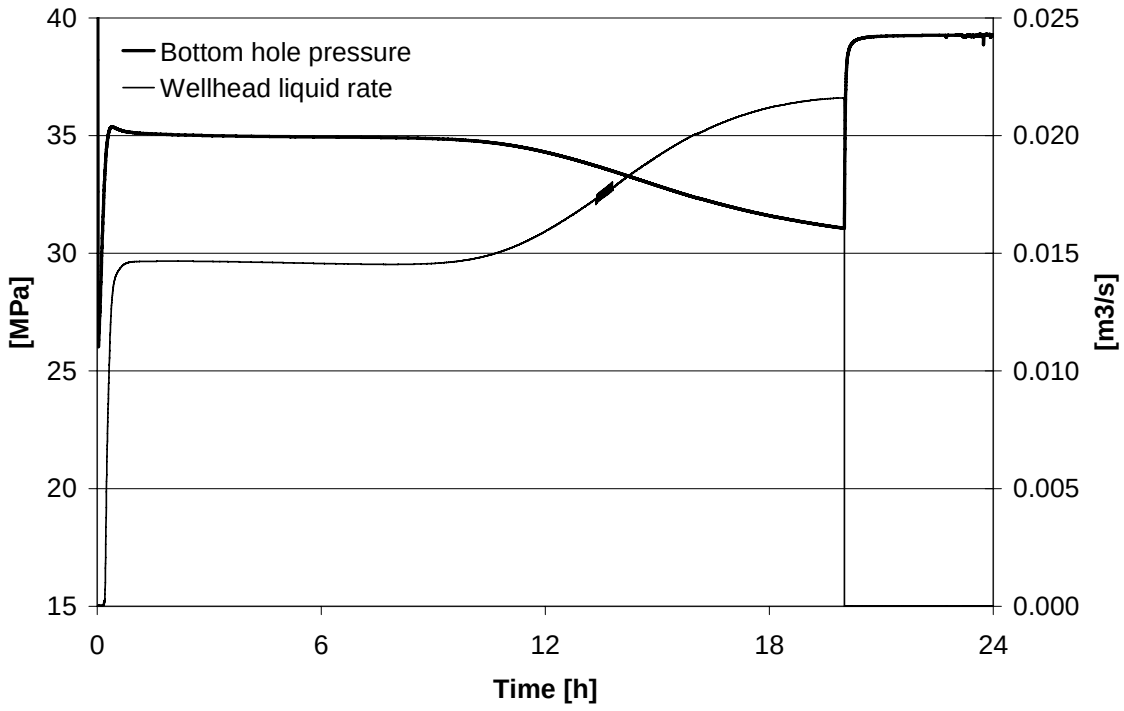

Figure 10. Bottomhole pressure and wellhead liquid rate.

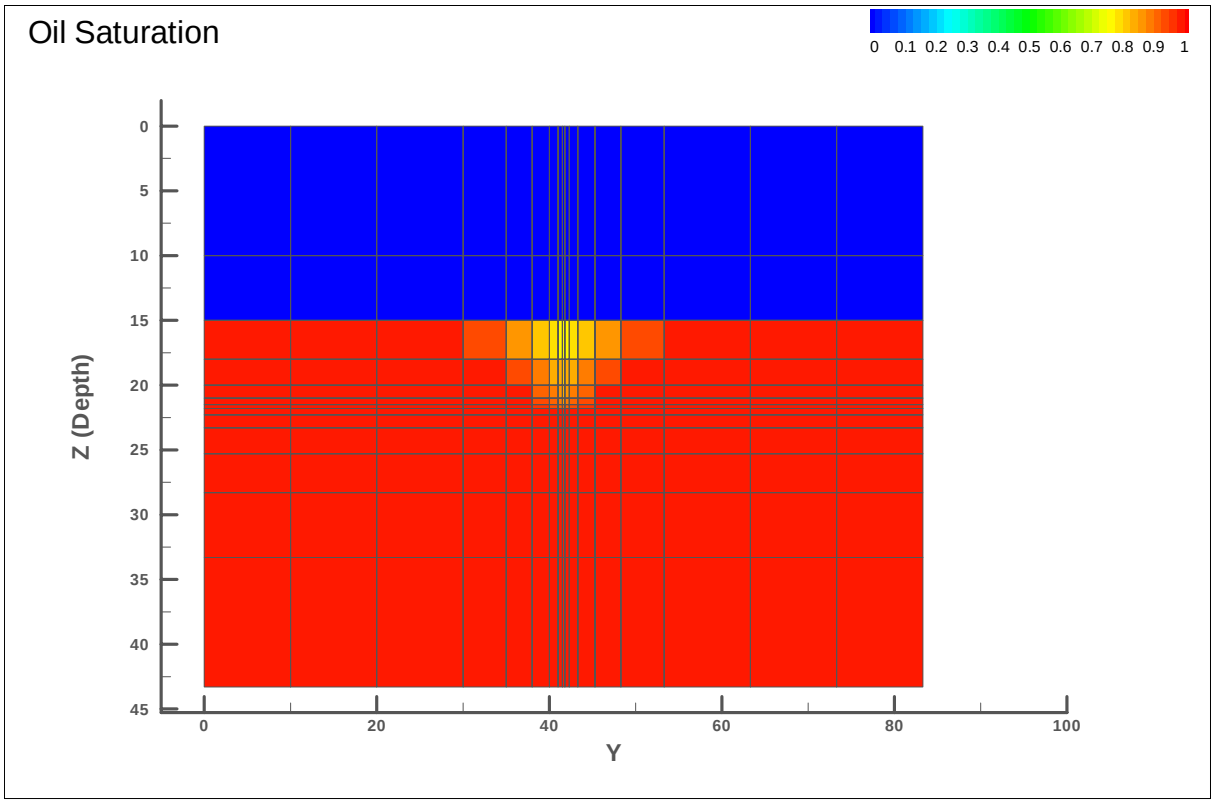

Figure 11. Cross section of reservoir oil saturation just before the shut-in.